Candidatus Nealsonbacteria (OD1) are biomass recycling ectosymbionts of methanogenic archaea in a stable benzene-degrading enrichment culture

Xu Chen[1], Olivia Molenda[1], Christopher T. Brown[2,3†], Courtney R. A. Toth[1], Shen Guo[1], Fei Luo[1††], Jane Howe[4], Camilla L. Nesbø[1], Christine He[5], Elizabeth A. Montabana[2,6], Jamie H. D. Cate[2,6,7], Jillian F. Banfield[5,6,8,9], and Elizabeth A. Edwards[1,*]

[1]Department of Chemical Engineering and Applied Chemistry, University of Toronto, Toronto, ON, M5S 3E5, Canada.
[2]Department of Molecular and Cell Biology, University of California, Berkeley, CA, USA
[3]California Institute for Quantitative Biosciences, University of California, Berkeley, CA, USA
[4]Department of Materials Science and Engineering, University of Toronto, Toronto, ON, M5S 3E4, Canada
[5]Innovative Genomics Institute, University of California, Berkeley, CA, USA
[6]Molecular Biophysics and Integrated Bioimaging, Lawrence Berkeley National Laboratory, Berkeley, CA, USA
[7]Department of Chemistry, University of California, Berkeley, CA, USA
[8]Department of Earth and Planetary Science, University of California, Berkeley, CA, USA;
[9]Environmental Science, Policy and Management, University of California, Berkeley, CA, USA;
†Current Address: Metagenomi, Inc., 1545 Park Avenue, Emeryville, CA, USA
††Current Address: Liven Proteins Corporation, 200 College Street, Toronto, ON, M5S 3E5, Canada.

Keywords: Candidate Phyla Radiation, Nealsonbacteria, genomics, genome-resolved metagenomics, fluorescent in situ hybridization, CryoEM, Benzene, Anaerobic, Methanothrix, methanogenic benzene biodegradation, biomass recycling

*Corresponding author mailing address: University of Toronto, Toronto, Ontario, M5S 3E5, Canada. Phone: (416) 946-0996. Fax: (416) 978-8605.
E-mail: elizabeth.edwards@utoronto.ca;

The authors declare no competing interests.

Summary

The Candidate Phyla Radiation (CPR) is a very large group of bacteria with no pure culture representatives, first discovered by metagenomic analyses. Within the CPR, candidate phylum Parcubacteria (previously referred to as OD1) within the candidate superphylum Patescibacteria is prevalent in anoxic sediments and groundwater. Previously, we had identified a specific member of the Parcubacteria (referred to as DGGOD1a) as an important member of a methanogenic benzene-degrading consortium. Phylogenetic analyses herein place DGGOD1a within the *Candidate* clade Nealsonbacteria. Because of its persistence over many years, we hypothesized that *Ca.* Nealsonbacteria DGGOD1a must serve an important role in sustaining anaerobic benzene metabolism in the consortium. To try to identify its growth substrate, we amended the culture with a variety of defined compounds (pyruvate, acetate, hydrogen, DNA, phospholipid), as well as crude culture lysate and three subfractions thereof. We observed the greatest (10 fold) increase in the absolute abundance of *Ca.* Nealsonbacteria DGGOD1a only when the consortium was amended with crude cell lysate. These results implicate *Ca.* Nealsonbacteria in biomass recycling. Fluorescent in situ hybridization and cryogenic transmission electron microscope images revealed that *Ca.* Nealsonbacteria DGGOD1a cells were attached to larger archaeal *Methanothrix* cells. This apparent epibiont lifestyle was supported by metabolic predictions from a manually curated complete genome. This is one of the first examples of bacterial-archaeal episymbiosis and may be a feature of other *Ca.* Nealsonbacteria found in anoxic environments.

26

27 ## Introduction

28 The candidate phylum Parcubacteria belongs to a superphylum referred to as the
29 Candidate Phyla Radiation (CPR) which was first defined by culture-independent metagenomic
30 analysis (1). Members of the CPR are phylogenetically diverse and ubiquitous, but are especially
31 abundant in lakes, sediment, and groundwater (1, 2). Although their roles are still not well
32 characterized, clues are emerging from the rapidly growing number of metagenome sequencing
33 projects and genome reconstructions. To date, most members of the Parcubacteria remain
34 uncultured and are only known from metagenome assembled genomes (MAGs). In 2020, Chen
35 *et al.* (3) summarized 38 closed, complete MAGs or cMAGs belonging to the CPR. As of 2022,
36 19 cMAGs from the Parcubacteria within the CPR can be retrieved from NCBI, but none is for a
37 member of the Nealsonbacteria subgroup. The genomes of Parcubacteria are extremely small (~1
38 Mb) and include many hypothetical proteins which lack homologs in well-studied microbes (4).
39 The reduced genomes of Parcubacteria encode few metabolic capacities, lacking the ability to
40 synthesize lipids and often missing complete pathways for the biosynthesis of several vitamins,
41 amino acids, and nucleotides (5, 6). Coupled with a lack of an electron transport system, the
42 small cells typical of Parcubacteria and other members of the CPR are thought to obtain nutrients
43 and energy through close contact with an obligate host or partner cell (7). Several recent
44 publications support this hypothesis. For example, Huddy et al. (8) inferred an association
45 between CPR member Saccharibacteria (TM7) and Actinobacteria based on abundance patterns.
46 He at el. (9) reveled episymbiotic interaction between ultrasmall cells and hosts in groundwater
47 by Cryo-TEM. Scanning transmission x-ray microscopy (STXM) data obtained by Alvarado et
48 al. (10) showed an association of ultra-small cells with filamentous bacteria which encapsulated

49 with elemental sulfur spherical granules. The most definitive study was a study of
50 Saccharibacteria (TM7) and its bacterial host, *Actinomyces odontolyticus* XH001, in cultivated
51 co-cultures (11). Saccharibacteria genomes share similarities with the Parcubacteria in that they
52 are small and lack complete biosynthetic pathways. Metagenomic analyses suggest that
53 Parcubacteria may also be closely associated with a host microbe, perhaps as an episymbiont (5,
54 9, 12, 13) but experimental evidence is scant because of the difficulty in cultivating and
55 enriching these tiny microorganisms from complex ecosystems.
56 Interestingly, a stable methanogenic benzene-degrading enrichment culture maintained in
57 our laboratory, referred to as the OR consortium (for Oil Refinery), provides an opportunity to
58 study a member of the Parcubacteria in vivo. The OR consortium was originally derived from
59 oil-contaminated sediments in 1995 and has since been maintained in anaerobic minimal
60 medium and provided with benzene as the only added electron donor and carbon source (14).
61 Multiple subcultures have been established over the years, including a scaled-up lineage
62 currently being used for bioaugmentation field trials (15-17). The dominant microbes in these
63 subcultures include specialized benzene-fermenting *Desulfobacterota* (ORM2), several
64 methanogenic archaea, and - most interestingly for this study - a member of the Parcubacteria
65 originally referred to as OD1 but now further classified as *Candidatus* Nealsonbacteria (Fig. S1)
66 in this study. The consortium repeatedly degrades benzene to methane and CO_2 at rates from 0.2
67 to 10 mg benzene/L/day, however the biochemical mechanism for anaerobic benzene
68 biodegradation is still poorly understood. Toth et al. (17) recently described the current state of
69 knowledge of the OR consortium, highlighting the coordinated metabolic interactions of ORM2
70 and acetoclastic and hydrogenotrophic methanogens for complete mineralization of benzene. *Ca.*
71 Nealsonbacteria might also play role in the OR consortium because they have consistently been

72 detected in every culture survey (18) although a clear correlation between the abundance of *Ca.*
73 Nealsonbacteria and benzene degradation rate has not been found. OR consortium cultures are
74 maintained in fed-batch mode with infrequent (every 1-2 months) shallow transfers into fresh
75 medium resulting in long cell residence times. Despite years of maintenance solely on benzene
76 the total microbial concentration remains below 10^9 cells/mL (19). Accumulated dead cells are a
77 likely an alternative carbon and energy source for microbial growth. More generally, *Ca.*
78 Nealsonbacteria are also found in anoxic hydrocarbon- and organohalide-contaminated sites (20,
79 21), high pH spring water (22), and other nutrient-limited groundwater environments (9), where
80 biomass turnover rates are sometimes high, perhaps in response to stress, therefore we
81 hypothesized that these microbes may play a role in biomass recycling.
82
83 We sought to identify the substrates of *Ca.* Nealsonbacteria and any possible host associations
84 within the benzene-degrading OR consortium using enrichment experiments on various
85 substrates, quantitative PCR (qPCR), sequencing and genome reconstruction, and various types
86 of microscopy. The most growth of *Ca.* Nealsonbacteria was seen in cultures amended with
87 crude cell lysate (prepared from the consortium itself or from *Escherichia coli*). Fluorescence *in*
88 *situ* hybridization (FISH) and electron microscopy (EM) revealed *Ca.* Nealsonbacteria as an
89 epibiont on the surface of *Methanothrix*, a methanogenic archaeon essential for completing the
90 biotransformation of benzene to methane. Hybrid assemblies of short read (Illumina) and long
91 read (PacBio) metagenomic sequences were used to successfully reconstruct the complete closed
92 genome of the uncultured Parcubacteria in OR consortium, designated DGGOD1a. This 1.16
93 Mbp genome displays biosynthetic deficiencies and other episymbiotic traits as observed in most
94 other Parcubacteria genomes. A maximum likelihood concatenated ribosomal protein tree

95 placed the DGGOD1a genome within the candidate group Nealsonbacteria (Figure S1) as
96 defined in Anantharaman et al. (23). These observations begin to shed light on uncharacterized
97 members of the CPR and bring into focus the phenomenon of bacterial episymbiosis on archaeal
98 hosts.
99

100 ## Results and Discussion

101 **qPCR reveals abundance of *Ca.* Nealsonbacteria in methanogenic cultures**

102 A qPCR survey of 15 different methanogenic benzene-degrading subculture bottles was
103 conducted to measure the abundance of benzene-fermenting *Desulfobacterota* ORM2 and *Ca.*
104 Nealsonbacteria (referred to as OD1 in previous studies), as well as the abundance of total
105 bacteria and total archaea. One subculture bottle named "OR-1bBig" was selected for use in two
106 substrate "Donor Trial" experiments because it contained a relatively high abundance of *Ca.*
107 Nealsonbacteria (~5% based on 16S rRNA amplicon sequencing results) and sufficient culture
108 volume was available (1.5 L). Other than benzene, the products of cell decay could feasibly
109 serve as electron donors in these bottles. This led us to hypothesize that components of lysed
110 cells might serve as growth substrates for *Ca.* Nealsonbacteria.
111

112 ***Ca.* Nealsonbacteria is most enriched in cultures amended with lysed cells.**

113 In Donor Trial #1, we tested three common substrates (pyruvate, acetate, and hydrogen), as well
114 as French-Press lysed benzene culture, and two specific components of cells (salmon sperm DNA,
115 and the phospholipid L-α-phosphatidylethanolamine) to see if any of these putative electron donors
116 could support the growth of *Ca*. Nealsonbacteria, directly or indirectly (Table S1). We found that
117 *Ca.* Nealsonbacteria concentrations increased in vials amended with lysed culture (Figure 1a). In

118 these vials, *Ca.* Nealsonbacteria relative abundance increased from 5% to 30% and absolute
119 abundance by an order of magnitude to 5.1×10^6 copies (cells)/mL over 4 months (Figure 1; data
120 in Table S2a). None of the other electron donors tested resulted in discernable enrichment of *Ca.*
121 Nealsonbacteria relative to benzene-amended controls. In bottles amended with pyruvate, *Ca.*
122 Nealsonbacteria absolute abundance increased ~5 times (up to 9.8×10^5 copies/mL), but relative
123 abundance decreased to 1% because other microbes grew much more (Figure 1b; Table S3). *Ca.*
124 Nealsonbacteria growth in pyruvate and acetate amended bottles may have resulted from the direct
125 substrate utilization or as an indirect consequence of cell growth and corresponding increase in
126 dead cells. Either way, neither pyruvate nor acetate were selective for *Ca.* Nealsonbacteria. As
127 expected, the abundance of benzene-degrading Desulfobacterota ORM2 dropped significantly in
128 the absence of benzene (Figure 1b). In the vials amended with cell lysate (second bar; Figure 1b),
129 in addition to enrichment of *Ca.* Nealsonbacteria to 30% of the population, we also observed
130 enrichment of *Syntrophaceae* while the absolute abundance of methanogenic archaea was
131 relatively stable (Table S2a). The ASV corresponding to *Syntrophaceae* was found to share 100%
132 16S RNA gene sequence identity to an uncultured *Syntrophaceae* (MH665869) from a
133 methanogenic pyrite forming culture fed with ferrous sulfide (FeS), H_2S, and CO_2 (24). A similar
134 metabolism may be occurring as our medium is reduced with FeS and buffered with bicarbonate
135 (25).
136
137 Nonmetric dimensional scaling (NMDS) was applied to further analyze Donor Trial #1 ASV data
138 (Figure S2a). The unfed "starved control" culture community clustered with communities from
139 culture vials amended with cell lysate, consistent with products of cell decay supporting the
140 microbial community in both cases. Methane production data from each treatment indicated that

141 the added substrate equivalents (chemical oxygen demand [COD]) were consumed by 4 months
142 (Table S4). Therefore, data collected at 7 months were from cultures that were starved for more
143 than 3 months and marked with "+" in the NMDS analysis. Interestingly, we found that after 7
144 months, the communities did not converge. We expected to see enrichment of *Ca.* Nealsonbacteria
145 in every vial after prolonged starvation. However, such enrichment was only clearly observed in
146 acetate and pyruvate-amended vials (Figure 2). Perhaps there was insufficient biomass growth,
147 therefore insufficient dead biomass in the other vials to detect enrichment of *Ca.* Nealsonbacteria.
148 Indeed, total cell concentrations were highest in acetate and sodium pyruvate amended vials.
149 Interestingly, a second ASV belonging to *Ca.* Nealsonbacteria (designated ASVb) was enriched
150 in the acetate- and pyruvate-amended cultures (Figure 2) and became more abundant than *Ca.*
151 Nealsonbacteria ASVa – the strain that is typically found in the benzene-degrading consortium
152 (18). These two *Ca.* Nealsonbacteria ASVs share only 91.2% 16S rRNA sequence identity. This
153 intriguing result suggests that different species may exhibit distinct preferences for the type of
154 lysed cell material they can metabolize, because the acetate- and pyruvate-amended cultures
155 selected for very different communities.
156
157 Building on the first trial, a second trial (Donor Trial #2) compared the growth of *Ca.*
158 Nealsonbacteria on lysates from the benzene culture as well as *E. coli* lysate. Further, we tested
159 three sub-fractions of the benzene culture lysate, which were separated by centrifugation and
160 tangential flow filtration with a 50kDa cut off as depicted in Figure S3. The pyruvate treatment
161 from Donor Trial #1 was also repeated but this time with added antibiotics (1 mM each kanamycin
162 and vancomycin) to try to increase selectivity for *Ca.* Nealsonbacteria. The results of Donor Trial
163 #2 (raw data in Table S2b) were similar to those of Donor Trial #1, with whole cell lysate resulting

164 in significant (>10×) growth (Figure S4) regardless of source (*E. coli* or benzene culture). At first
165 glance, the *E. coli* crude lysate appeared to be most stimulatory, but we later realized it was
166 provided at 10× the concentration of the lysate from the benzene culture based on measured COD
167 (Table S1c). The fact that *E. coli* lysate also supported the growth of *Ca.* Nealsonbacteria ruled
168 out involvement of culture specific substrates (e.g., archaeal lipids). The sub-fractions of benzene
169 culture lysate also resulted in enrichment although we observed considerable variability between
170 duplicates (Figure S4). Of the three cell lysate fractions, the >50 kDa fraction (supernatant
171 retentate) was most effective at enriching *Ca.* Nealsonbacteria after 4 months of incubation which
172 may suggest that larger molecules may be important for growth. An NMDS analysis was also
173 conducted on amplicon sequencing data from Donor Trial #2 (Figure S2b). These results show
174 that the microbial communities enriched on each fraction of benzene culture lysate were slightly
175 different after the first two months (triangles), but that they converged after four months (squares).
176 Perhaps after four months, only larger, more slowly degraded biomolecules remained in all
177 fractions and results in similar communities.
178
179 To look more closely at the microbial composition in each treatment, a heatmap of absolute
180 abundance was generated showing the top 18 ASVs in Donor Trial #2 (Figure 3); raw data are
181 reported in Table S5. *Ca.* Nealsonbacteria ASVa was the most abundant sequence variant detected.
182 Only two other microbes (*Methanothrix* and *Spirochaetaceae)* were consistently enriched with *Ca.*
183 Nealsonbacteria in vials amended with cell lysate, regardless of source or sub-fraction tested. Vials
184 amended with lysed *E. coli* also enriched for ASVs belonging to *Clostridium* and *Bacteroides* that
185 were not enriched in other treatments (Figure 3). Comparing the culture amended with only
186 pyruvate in Donor Trial #1, the vials amended with antibiotics kanamycin and vancomycin

187 successfully inhibited the growth of most microbes including *Ca.* Nealsonbacteria and
188 *Methanothrix.* This indicates that *Ca.* Nealsonbacteria is antibiotic-sensitive or indirectly affected
189 by its antibiotic-sensitive metabolic partners. It is interesting to note that the culture's benzene
190 fermenter (ORM2) seems to have persisted in those treatments. The growth of
191 *Methanomethylovorans* and *Methanobacterium* in the presence of antibiotics confirms their
192 resistance and together these data point to a possible means of enriching for benzene-degrading
193 *Desulfobacterota* ORM2.
194
195 The two donor trials confirmed that compound(s) present in bacterial cell lysate can enrich *Ca.*
196 Nealsonbacteria. The exact identity of the compound(s) remains elusive, but the data point to
197 higher molecular weight and/or more recalcitrant proteins or extracellular polymeric substances,
198 as these would present in all of the fractions tested. Two very distinct strains of *Ca.*
199 Nealsonbacteria grew in the culture depending on treatment revealing subtle ecological
200 preferences yet to be discovered.
201
202 **Fluorescence in situ microscopy (FISH) reveals *Ca.* Nealsonbacteria DGGOD1a as an**
203 **epibiont of *Methanothrix*.**
204 To visualize the enriched *Ca.* Nealsonbacteria in the methanogenic benzene degrading culture by
205 microscopy, we attempted to develop specific mono-fluorescent *in situ* hybridization (FISH)
206 probes targeting various single stranded regions in the 16S rRNA gene. However, none of the
207 probes worked, possibly because of low ribosome counts in these cells (26) or non-ideal targeting
208 in the secondary structure. Very recently, Kuroda et al. (27) successfully designed and validated a

209 mono-FISH probe for a *Ca.* Nealsonbacteria with a nearly identical 16S RNA gene sequence by
210 targeting a different location on the gene; clearly this new FISH probe will be tested in the future.
211
212 As an alternative to a *Ca.* Nealsonbacteria-specific FISH probe, we used a combination of a
213 universal Archaea FISH probe (ARCH915, Table S6) and DAPI staining to distinguish
214 methanogens from bacteria. Given that *Ca.* Nealsonbacteria DGGOD1a was the most abundant
215 bacterial phylotype in several of our lysate-amended enrichment cultures (Figure 3), we compared
216 microscopic cell counts to qPCR abundance estimates of the same sample to confirm that the ultra-
217 small cells were *Ca.* Nealsonbacteria. We focused primarily on one specific cell lysate enrichment
218 culture (Lysate replicate #2 at 2 months) because of its high *Ca.* Nealsonbacteria abundance (>10^6
219 cells/mL in this culture compared to all other bacterial phylotypes (Figure 3). In this *culture*, we
220 observed many DAPI-stained ultra-small (~0.2 μm) cells attached to a single filamentous structure
221 that stained with the archaeal FISH probe (Figure 4a). The ultra-small cell size matches the typical
222 size of CPR members (5, 9) and is presumed to be *Ca.* Nealsonbacteria. The shape of the
223 filamentous archaea is distinctive of *methanothrix* cells. We counted the number of small cells
224 attached to long archaeal filaments as well as the number of filamentous archaea. We also counted
225 the number of free-living microbes with similar size and shape to that of the attached small cells.
226 Twenty-one fields of view were imaged and counted for each of two independent samples from a
227 *Ca.* Nealsonbacteria enrichment culture. These small cells were by far the most numerous bacteria
228 in all views, and thus must correspond to *Ca.* Nealsonbacteria, as it was most numerous via qPCR
229 in this culture. The count of small *Ca.* Nealsonbacteria cells was 3.2-6.6×10^6 cells /ml with
230 attached cells ~2.5 times more abundant than free-living cells. (Table S7). Gene copies by qPCR
231 in samples of DNA extracted from the same culture using primers specific for *Ca.* Nealsonbacteria

232 gave a comparable result of 8.3×10^6 copies/ml. Thus, we are confident that the small cells attached
233 to the archaeal filaments are *Ca.* Nealsonbacteria. *Methanothrix* cell counts were also estimated at
234 $1.9\text{-}3.4\times10^6$ cells/mL, which also matches reasonably well to the value of 0.9×10^6 cells/mL from
235 qPCR results (Table S7). Interestingly, a similar association of *Ca.* Patescibacteria and
236 *Methanothrix* was very recently reported in an artificial mixture of a culture of *Methanothrix*
237 *soehngenii* GP6 with wastewater biosludge (27).
238
239 We had previously unsuccessfully attempted to enrich *Ca.* Nealsonbacteria by filtration through a
240 0.22-µm filter. Analysis of the filtrate by qPCR showed no enrichment: both bacterial and the *Ca.*
241 Nealsonbacteria concentrations decreased 100-fold (data not shown). Other studies have reported
242 success enriching ultra-small microbes this way (1, 26, 28). Perhaps the strong attachment of *Ca.*
243 Nealsonbacteria to its host caused this approach to fail. Interestingly, we also noticed that the
244 archaeal FISH probe seemed to bind more strongly to methanogens that had many *Ca.*
245 Nealsonbacteria cells attached, compared to naked methanogens (Figure 4a, bottom right; Figure
246 S5). Naked methanogens stained brightly with DAPI (DNA) but only faintly with the archaeal
247 FISH probe (rRNA). Given that FISH signal intensity is a measure of ribosome count and thus
248 metabolic activity (29), perhaps methanogens with *Ca.* Nealsonbacteria attached are more active.
249 This observation is in contrast to the recent study by Kuroda et al., (27) where a major fraction of
250 the Ca. Nealsonbacteria were attached to methanogens with weaker fluorescence. *Ca.*
251 Nealsonbacteria's role as either a parasitic or commensal organism is thus still unclear.
252
253 **SEM and Cryo-EM confirm attachment to *Methanothrix*.**

254 SEM examination of the parent methanogenic benzene-degrading culture prepared with ionic
255 liquid exchange to preserve cell structure also showed a similar association of very small *Ca.*
256 Nealsonbacteria-like cells attached to a large filamentous cell structure consisting of a chain of
257 rod-shaped, blunt-ended cells (Figure 4b). This filament was enclosed in a tubular sheath and the
258 flat ends distinctively match the characteristics of *Methanothrix* (30). The *Ca.* Nealsonbacteria-
259 like cells are spherical with a diameter of 0.2 µm to 0.8 µm and they were always found in budding
260 pairs, forming a peanut shape. Cryo-EM was also used to examine the *Ca.* Nealsonbacteria
261 enrichments. The Cryo-EM images (Figure 4c) show the same association of peanut-shaped cells
262 with *Methanothrix*. The large black rod-shaped blurry cells at the center of the image are
263 *Methanothrix* forming a sheathed chain. Multiple peanut-shaped ultra-small cells were observed
264 attached to the chain of *Methanothrix* (Figure 4c). The *Ca.* Nealsonbacteria-like cells were always
265 found in pairs and the one attached to the methanogen was usually bigger. A zoomed-in image
266 (Figure 4c; right side) reveals that *Ca.* Nealsonbacteria cells have a very interesting membrane
267 structure with a thick sheath and an apparent S-layer. Additional supporting FISH, SEM, Cryo-
268 EM images are provided in Figures S5 and S6. The close association of *Ca.* Nealsonbacteria and
269 *Methanothrix* may facilitate efficient nutrient exchange between these organisms. Given that
270 *Methanothrix* are obligate acetoclastic methanogens, *Ca.* Nealsonbacteria may provide acetate to
271 *Methanothrix*. The physical association also enables potential direct interspecies electron transfer
272 or DIET (31). Although, e-pili genes were not found in the *Ca.* Nealsonbacteria genome (see
273 below), DIET or direct acetate exchange could happen by other mechanisms. Clearly the possible
274 syntrophy between the *Ca.* Nealsonbacteria and *Methanothrix* requires further investigation.
275

276 **A co-occurrence network finds *Ca.* Nealsonbacteria variants positively correlated with**
277 ***Methanothrix*.**
278 A co-occurrence network inference (CoNet) analysis was conducted using all 16S rRNA amplicon
279 sequencing data from the two donor trials (Figure S7a). *Ca.* Nealsonbacteria ASVa was found to
280 correlate positively with its putative host *Methanothrix* ASV89, as well as to *Ca.* Nealsonbacteria
281 ASVb and to two less abundant microbes (*Sporomusa* and *Ignavibacteriales*) and to correlate
282 negatively with *Spirochaetaceae* ASV977, which was only enriched in the bottles amended with
283 pyruvate. *Ca.* Nealsonbacteria ASVb (enriched only when pyruvate or acetate were added) was
284 positively correlated with *Methanothrix* ASV89 as well as to *Methanothrix* ASV91. ASV91 shares
285 99.4% pairwise identity with *Methanothrix* ASV89 and could be a specific host for *Ca.*
286 Nealsonbacteria ASVb. A heatmap of absolute abundance was generated (Figure S7b) that
287 includes all the ASVs from the co-occurrence network. The rows of heatmap were clustered based
288 on similarity. Interestingly, *Ca.* Nealsonbacteria ASVa clustered with *Methanothrix* ASV89 while
289 *Ca.* Nealsonbacteria ASVb clustered with *Methanothrix* ASV91 (Figure S7b, red rectangles). This
290 clustering suggests that *Ca.* Nealsonbacteria ASVa and ASVb may have different *Methanothrix*
291 hosts.
292
293 **Impact of *Ca.* Nealsonbacteria on benzene degradation**
294 To further study the role of *Ca.* Nealsonbacteria in benzene degradation, we mixed an enrichment
295 (containing about 10^7 *Ca.* Nealsonbacteria cells/mL) with a "slow" benzene-degrading culture
296 (containing about 10^7 ORM2 cells/mL, degrading at ~0.1 mg/L/day). As a control, we also
297 amended the slow culture with supernatant recovered from a healthy culture (degrading benzene
298 at 10 mg/L/day). The raw data from this experiment are reported in Table S8. We observed a

299 significant increase in benzene degradation rate in the two replicates that were a 50:50 mix of the
300 two cultures (Figure 5a), even though mixing diluted the benzene degrader (ORM2) by 50%.
301 Therefore, adding a *Ca.* Nealsonbacteria enrichment enhanced benzene degradation. Slow benzene
302 culture amended with supernatant from a healthy culture as well as the slow culture-only controls
303 all showed overall slower benzene degradation (Figure 5a). Benzene biodegradation rates were
304 highest in cultures with the highest measured ORM2 concentrations at Day 217, except for one
305 culture replicate (slow culture #1) with abundant ORM2 but no benzene degradation activity
306 (Figure 5b). The two vials amended with the *Ca.* Nealsonbacteria enrichment showed the highest
307 cell concentrations for both ORM2 and *Ca.* Nealsonbacteria. Perhaps *Ca.* Nealsonbacteria
308 supplied ORM2 or *Methanothrix* with specific limiting metabolites, nutrients or cofactors recycled
309 from lysed biomass or simply removed inhibitory compounds. Further studies using isotope-
310 labeled cell lysate may help to clarify these complex interactions.
311

312 **The genome of *Ca.* Nealsonbacteria DGGOD1a is consistent with a symbiotic epibiotic**
313 **lifestyle**

314 We assembled and closed the genome of *Ca.* Nealsonbacteria DGGOD1a (Genbank: CP092821
315 and IMG ID: 2791354853) corresponding to ASVa using both Illumina and PacBio sequence data.
316 The details of assembly are summarized in Supplemental Text S4 and reported in a genome
317 announcement (55). The quality of the genome assembly was validated with read-mapping and a
318 GC skew plot (Figure S8) clearly showing origin and terminus. The complete genome is 1.16 Mbp
319 in length with 1173 predicted coding sequences (CDS) including 18 pairs of perfect repeats which
320 are over 400 bp in length. The majority of these repeats are predicted transposases, and in fact, this
321 genome has a total of 39 predicted transposases which comprise 3.4% of protein coding genes.

322 Transposases are involved in genomic rearrangements, gene duplication and for promoting
323 horizontal gene transfer (32). A total of nine regions were predicted as genomic islands using
324 Islandviewer4 (31) of which seven contain transposases (Table S9). High numbers of transposases
325 are found in organisms under stress or in extreme environments (32) which may explain the
326 unusual high decay rate sometimes seen in our methanogenic benzene degrading culture (19).
327 Other studies have also shown a high transposase content in bacteria with symbiotic or pathogenic
328 lifestyles (33-35). The transposases in the genome of *Ca.* Nealsonbacteria may participate in DNA
329 exchange with the host *Methanothrix.*
330
331 Like other CPR bacteria, the genome reveals that most metabolic pathways and biosynthetic
332 capacities annotated by automatic pipelines are predicted to be incomplete, notably of nucleotides,
333 lipids, vitamins and most amino acids (Figure 6). As inferred from genomes of other members of
334 the CPR group (1, 5, 7), DGGOD1a can use the pentose phosphate pathway to bypass glycolysis.
335 Also, there is no lipid biosynthesis pathway and the pathways for the biosynthesis of most amino
336 acids and vitamins are incomplete. The only vitamin DGGOD1a is predicted to make is riboflavin.
337 The large ribosomal RNA subunit L1 is missing; a common feature of members of the OD1-L1
338 group (1, 5). Interestingly, eight toxin and five antitoxin gene families were found in the genome.
339 Some were found located within two predicted genomic islands and may contribute to their
340 maintenance (36). The toxin-antitoxin systems are stress-response elements that could also help
341 cells adapt to unfavorable growth conditions (36). These systems are common in free-living
342 microbes but tend to be lost from host-associated prokaryotes due to the relatively constant
343 environment of host-associated organisms (37). The high toxin-antitoxin genes copies in *Ca.*
344 Nealsonbacteria indicates that it is possibly still undergoing reductive evolution (36, 38). Twelve

345 type IV pilus assembly proteins, two cell membrane proteins annotated as holins, and type II
346 secretion system genes were found in the genome, which are consistent with an epibiont lifestyle.
347 Epibionts are known to use type IV pili to attach to the host membrane (39). The holin protein
348 family form pores in cytoplasmic membranes and may be used to permeabilize the host cell
349 membrane and perhaps kill the host (40). Type II secretion systems may be involved in nutrient
350 uptake or nutrient exchange between the *Ca.* Nealsonbacteria and its host and may also participate
351 in DIET (41). Surprisingly, a type V CRISPR-Cas system that contains 49 spacers was found in
352 the genome with Cas12a as the effector and the complex of cas4, cas1 and cas2 as the spacer
353 acquisition machinery. It is rare to see a CRISPR-Cas system in such a reduced genome, and only
354 2.4% of organisms from the Parcubacteria and Microgenomates superphyla have a CRISPR-Cas
355 system (42). The intact CRISPR-Cas system suggests exposure to phage and extracellular DNA.
356 Considering that *Ca.* Nealsonbacteria lack the ability to synthesize nucleotides, perhaps the
357 CRISPR-Cas system is involved in the degradation of host DNA for recycling nucleotides. No
358 clues were gleaned from a search of CRISPR spacer targets against the OR consortium
359 metagenome and all the sequences in the NCBI database, as these searches only returned hits to
360 the CRISPR matrix itself.
361
362 We were not able to assign function to a large proportion (30%) of the predicted proteins in the
363 genome, despite running multiple prediction pipelines and manual curation (Table S10). One
364 interesting feature is a putative NADP-reducing hydrogenase. This protein has been found in the
365 bacterium *Desulfovibrio fructosovorans* as an iron-sulfur protein that exclusively functions as a
366 hydrogen dehydrogenase (43) and may mean that Ca. Nealsonbacteria uses hydrogen produced by
367 other fermentation reactions. The genome also encoded two putative polysaccharide deacetylases

368 belonging to carbohydrate esterase family 4 (CE4). The members of this family can hydrolyze the
369 acetyl group from *N*-acetylglucosamine (44-47) or *O*-acetylxylose residues (48, 49) which exist in
370 extracellular polymeric substances (EPS). The released acetyl group could be used by the obligate
371 acetoclastic methanogenic archaeon *Methanothrix*. Three genes encoded putative peptidoglycan-
372 binding proteins were also found in the genome. The proteins belong to peptidoglycan-binding
373 domain could involve in cell wall synthesis (50) and binding (51) which may responsible for the
374 complex membrane structure we found by Cryo-EM.
375
376 **Implications**
377 *Ca.* Nealsonbacteria DGG1a likely contributes to recycling biomass including extracellular
378 polymeric substances in a methanogenic benzene degrading enrichment culture, and in so doing
379 enhances the growth of benzene fermenters. A role in microbial biomass recycling is supported by
380 substantial enrichment of this phylotype on lysed biomass. The finding of a close association of
381 dividing *Ca.* Nealsonbacteria cells with *Methanothrix* is now the second report of a CPR bacterium
382 that is an episymbiont of an archaeon (27), in this study shown in a stable laboratory enrichment
383 culture where further experimentation is possible. *Ca.* Nealsonbacteria were observed to be
384 beneficial for the growth of benzene-metabolizing *Desulfobacterota* ORM2 from yet another
385 uncultivated lineage. *Ca.* Nealsonbacteria may recycle key cofactors required to initiate benzene
386 ring activation. These results guide future experiments into specific relationships between *Ca.*
387 Nealsonbacteria and benzene degradation in these enrichment cultures.
388
389 The visualization of this unusual cross-kingdom episymbiosis of *Ca.* Nealsonbacteria on the
390 surface of *Methanothrix* implies metabolite exchange or direct electron transfer between the two

391 cell types. The type IV pili encoded in the genomes of many *Ca.* Nealsonbacteria (5, 7, 52) are
392 possibly used for attachment to the host and as well as a conduit for electron transfer. Perhaps
393 these tiny microbes revealed in many metagenomic surveys of natural and engineered anaerobic
394 communities have analogous roles? *Ca.* Nealsonbacteria may be particularly relevant where
395 energy input is limited and recycling is vital, such as in deep subsurface environments.
396

397 ## Experimental Procedures

398 **Chemicals and microbial cultures.** All chemicals were obtained from Sigma-Aldrich (Oakville,
399 ON, Canada) at the highest purity available unless specified otherwise. The OR consortium is
400 maintained in 100 mL to 2 L batch culture bottles at the University of Toronto and in larger vessels
401 (>100 L) at SiREM laboratories (Guelph, Ontario, Canada); the scaled-up culture is referred to as
402 DGG-B (17). Two OR consortium subculture bottles (or lineages) were used in the experiments
403 described herein: a bottle called OR-1bBig was the inoculum for *Ca.* Nealsonbacteria enrichment
404 Donor Trials #1 & #2 and a bottle called OR-p5 was the inoculum for the augmentation
405 experiment. All cultures were grown in an iron sulfide (FeS)-reduced, bicarbonate-based mineral
406 medium (MM medium) amended regularly (approx. 1 per month) with benzene targeting aqueous
407 concentration of 10 mg/L per bottle (17, 18).
408

409 **Preparation of electron donor solutions for *Ca.* Nealsonbacteria enrichment trials.** Two
410 crude cell lysate solutions from the OR consortium OR-1bBig and a culture of *Escherichia coli*
411 were prepared using tangential flow filtration and French press as described in Text S1. Next, we
412 prepared two solutions of specific biomass components, nucleic acids (salmon sperm DNA;
413 Sigma-Aldrich, Deoxyribonucleic acid sodium salt) and a membrane lipid (L-α-

414 phosphatidylethanolamine; Sigma-Aldrich, Type II, ≥97%, lyophilized powder from egg yolk).
415 Acetate, pyruvate and hydrogen were also tested as donors as they are intermediates of benzene
416 degradation. Stock solution concentrations are listed in Table S1a.
417
418 ***Ca.* Nealsonbacteria Enrichment – Donor Trial #1.** To test if *Ca.* Nealsonbacteria DGGOD1a
419 could grow on crude lysed biomass or specific sub-cellular components, 25 mL culture tubes with
420 9 mL MM medium were inoculated with 1 mL OR-1bBig culture and amended with 7 different
421 electron donor solutions (Table 14a) at approximately the same electron equivalents, targeting ~30
422 mg COD/L. Each condition was tested in quadruplicate and incubated in a Coy anaerobic glove
423 box for 7 months (supplied with 10% H_2, 10% CO_2, and 80% N_2). DNA samples were collected
424 at 2, 4, and 7 months after inoculation by sacrificing an entire replicate from each treatment.
425
426 ***Ca.* Nealsonbacteria enrichment – Donor Trial #2.** After observing successful growth and
427 enrichment of *Ca.* Nealsonbacteria with crude cell lysate from the benzene culture in Donor Trial
428 #1, a second experiment was set up to test the impact of various biomass fractions of cell lysate.
429 Culture (500 mL) was concentrated by tangential flow and cells were lysed using the same French
430 press method described earlier (Text S1). The cell lysate was then divided into four fractions, as
431 seen in Figure S3. One fraction was used "as is" (BL for Benzene culture Lysate). The remaining
432 lysate was centrifuged (at 13,000 × g for 20 mins) to create a pellet fraction and a supernatant
433 fraction. The supernatant fraction was further separated by tangential flow filtration with 50kDa
434 cut-off membrane (Pellicon® XL cassette with Durapore® membrane) to create a permeate fraction
435 (< 50 kDa) and a retentate fraction (>50 kDa). Each of these fractions was tested separately (Table
436 S1b). Two additional treatments were included in Donor Trial #2. One consisted of pyruvate plus

437 the antibiotics kanamycin and vancomycin (1 mM) to inhibit bacteria without inhibiting
438 methanogens. A second additional treatment was amended with *E. coli* extract instead of benzene
439 culture extract. We ensured that the *E. coli* pellet was well washed with MM medium to remove
440 any residual *E. coli* rich growth medium that could confound results. Controls without substrate
441 (starved control; SC) and crude benzene culture lysate without inoculum (no inoculum; NI) were
442 included. All treatments were conducted in biological duplicates except the starved control which
443 was a singleton.
444
445 ***Ca.* Nealsonbacteria augmentation trial.** This experiment made use of an inoculum from culture
446 bottle "OR-p5" with a very slow benzene degradation rate over years (~0.1 mg/L/day). Eight 25-
447 mL culture vials were each filled with a 10 mL aliquot of this slow culture (see Text S2 for details).
448 Subsequently, 5 mL of OR-p5 culture was removed from vials #1-2 and replaced with 5 mL of *Ca.*
449 Nealsonbacteria enrichment culture BL (replicate #1) from Donor Trial #2. In vials #3-5, 5 mL of
450 culture was removed and replaced with 5 mL of culture supernatant from a very active benzene
451 culture (degradation rate of ~10 mg/L/day), prepared by centrifugation at 13,000 × g for 20 min.
452 The remaining vials (#6-8) of slow culture were left as is. All vials were amended with neat
453 benzene targeting 15 mg/L aqueous concentration and reamended whenever concentrations
454 decreased below 5 mg/L. Benzene and methane concentrations were monitored by GC/FID (see
455 below). DNA samples were collected on day 217 for qPCR analysis.
456
457 **DNA extraction, quantitative PCR, and Illumina amplicon sequencing and statistical**
458 **analysis.** DNA from Donor Trial #1 was extracted from 10 mL culture samples; otherwise, DNA
459 was extracted from 1 mL culture samples. Cells were harvested by centrifugation at 13,000 × g for

460 20 min at 4°C and pellets resuspended in residual (~0.05 mL) supernatant. DNA was extracted
461 using the DNeasy PowerSoil Kit (QIAGEN) following the manufacturer's protocol. Real-time
462 quantitative polymerase chain reaction (qPCR) assays were performed to track the gene copy
463 numbers of Bacteria and Archaea using universal 16S rRNA gene primers; abundances of *Ca.*
464 Nealsonbacteria and *Thermodesulfobacteria* ORM2 were also tracked using specific 16S rRNA
465 gene-targeting primers (Table S11). qPCR reactions were performed using a CFX96 real-time
466 thermal cycler (Bio-Rad Laboratories) using the following thermocycling conditions: an initial
467 denaturation step at 98 °C for 2 min, 40 cycles of 98 °C for 5 s and Tm (see Table S11) for 10 s,
468 followed by melt curve analysis (65-95 °C with an increase of 0.5 °C every 5 s). qPCR results
469 were processed with CFX Manager software (Bio-Rad Laboratories). Standard curves for all the
470 qPCR studies are reported in Table S12. 16S rRNA gene amplicon sequencing with primers
471 targeting the V6-V8 region was conducted at the Genome Quebec Innovation Centre (McGill
472 University) as previously described (17). Raw reads were processed into amplicon sequence
473 variants (ASVs) and analyzed by nonmetric dimensional scaling (NMDS) and Co-occurrence
474 Network Inference (CoNet) analysis (53) as described in Text S3.
475
476 **Metagenome analysis.** The OR consortium/DGG culture was sequenced using a combination of
477 Illumina paired-end (~150 bp reads, ~300 bp insert) and PacBio long-read library (~7000 bp
478 reads). Metagenomes were submitted to IMG under sequencing project Gp0324998. Detailed
479 description of assembly, binning and functional and taxonomic annotation can be found in Text
480 S4.
481

482 **Epifluorescence microscopy and fluorescence in situ hybridization (FISH).** The FISH probe
483 ARCH915 was used for visualizing all Archaea (54). Eight FISH probes (Table S6) targeting the
484 16S rRNA gene of *Ca.* Nealsonbacteria were designed and tested in this study but none yielded a
485 signal distinguishable from background noise. The protocol for epifluorescence microscopy is
486 provided in Text S5 and details into the design and testing of FISH probes in Text S6.
487
488 **Scanning Electron Microscopy with Ionic Liquid and Cryo-EM.** To maintain the wet native
489 state of microbial cells and to eliminate artifacts that may be introduced by sample drying and
490 coating, culture samples were prepared with an ionic liquid and examined by SEM, as detailed in
491 Text S7. Cryo-EM was also used to explore intracellular structure and spatial associations. Sample
492 preparation and Cryo-EM conditions are described in Text S8.
493
494 **Analytical procedures.** Benzene and methane were measured in culture bottles and vials by
495 injecting 0.3 mL headspace samples into a Hewlett-Packard 5890 Series II GC fitted with a GSQ
496 column (30 m x 0.53 mm I.D. PLOT column; J&W Scientific, Folsom, CA) as previously
497 described (18). External standards were used for calibration.
498
499 **Accession numbers.** The closed genome sequence of *Candidatus* Nealsonbacteria DGGOD1a is
500 available at the Joint Genome Institute (IMG) under Taxon ID 2791354853 and at NCBI under
501 accession no. CP092821. Amplicon sequences (16S rRNA) were uploaded to the NCBI SRA under
502 BioProject accession number PRJNA830497. The Genome is also available in ggkbase with the
503 following link: https://ggkbase.berkeley.edu/organisms/410827/contigs/251537015.
504

505 **Supporting information**

506 The PDF file contains: 1) supplementary Figures S1 to S6, including a phylogenomic tree of *Ca.*
507 Nealsonbacteria, fractionation steps used to preparer biomass, NDMS plots, *Ca.* Nealsonbacteria
508 growth curves and additional microscopic images; 2) supporting texts (S1 to S8) providing
509 additional method details; and 3) supplementary Tables S9, S10, S11 listing primers, probes and
510 qPCR standard curves. The excel file contains larger data Tables S1 and S5-S12.

511

512 **Acknowledgements**

513 This study was funded by Genomic Application Partnership Program (GAPP) grants awarded to
514 E.A.E. (Project IDs OGI-102 and OGI-173), which were supported by Genome Canada, Ontario
515 Genomics, the Government of Ontario, Mitacs Canada, SiREM, Alberta Innovates, Federated Co-
516 operatives Limited, and Imperial Oil. The authors would like to thank SiREM (Guelph, Ontario
517 N1G 3Z2, Canada) for supplying culture for testing. We would also like to acknowledge the
518 laboratories of Dr. Neil Thomson (University of Waterloo), Dr. Ania Ulrich (University of
519 Alberta), SiREM, and Innotech Alberta (Edmonton, Alberta T6N 1E4, Canada) for providing
520 feedback and intellectual contributions to this study during weekly GAPP consortium meetings.

521

522 **References**

523 1. Brown CT, Hug LA, Thomas BC, Sharon I, Castelle CJ, Singh A, Wilkins MJ, Wrighton KC,
524 Williams KH, Banfield JF. 2015. Unusual biology across a group comprising more than 15% of
525 domain Bacteria. Nature 523:208-11.

526 2. Hug LA, Baker BJ, Anantharaman K, Brown CT, Probst AJ, Castelle CJ, Butterfield CN,
527 Hernsdorf AW, Amano Y, Ise K, Suzuki Y, Dudek N, Relman DA, Finstad KM, Amundson R,
528 Thomas BC, Banfield JF. 2016. A new view of the tree of life. Nat Microbiol 1:16048.

529 3. Chen L-X, Anantharaman K, Shaiber A, Eren AM, Banfield JF. 2020. Accurate and complete
530 genomes from metagenomes. Genome Research 30:315-333.

531 4. Méheust R, Burstein D, Castelle CJ, Banfield JF. 2019. The distinction of CPR bacteria from other
532 bacteria based on protein family content. Nature Communications 10.

533 5. Castelle CJ, Brown CT, Thomas BC, Williams KH, Banfield JF. 2017. Unusual respiratory
534 capacity and nitrogen metabolism in a Parcubacterium (OD1) of the Candidate Phyla Radiation. Sci
535 Rep 7:40101.

536 6. Wrighton KC, Thomas BC, Sharon I, Miller CS, Castelle CJ, VerBerkmoes NC, Wilkins MJ,
537 Hettins RL, Lipton MS, Williams KH, Long PE, Banfield JF. 2012. Fermentation, hydrogen, and
538 sulfur metabolism in multiple uncultivated bacterial phyla. Science 337:1661-1665.

539 7. Nelson WC, Stegen JC. 2015. The reduced genomes of Parcubacteria (OD1) contain signatures of a
540 symbiotic lifestyle. Front Microbiol 6:713.

541 8. Huddy RJ, Sachdeva R, Kadzinga F, Kantor RS, Harrison STL, Banfield JF. 2021. Thiocyanate and
542 Organic Carbon Inputs Drive Convergent Selection for Specific Autotrophic Afipia and
543 Thiobacillus Strains Within Complex Microbiomes. Frontiers in Microbiology 12.

544 9. He C, Keren R, Whittaker ML, Farag IF, Doudna JA, Cate JHD, Banfield JF. 2021. Genome-
545 resolved metagenomics reveals site-specific diversity of episymbiotic CPR bacteria and DPANN
546 archaea in groundwater ecosystems. Nat Microbiol 6:354-365.

547 10. Alvarado LEV, Fakra SC, Probst AJ, Giska JR, Jaffe AL, Oltrogge LM, West-Roberts J, Rowland
548 J, Manga M, Savage DF, Greening C, Baker BJ, Banfield JF. 2022. Autotrophic biofilms sustained
549 by deeply-sourced groundwater host diverse CPR bacteria implicated in sulfur and hydrogen
550 metabolism doi:10.1101/2022.11.17.516901. Cold Spring Harbor Laboratory.

551 11. He X, McLean JS, Edlund A, Yooseph S, Hall AP, Liu SY, Dorrestein PC, Esquenazi E, Hunter
552 RC, Cheng G, Nelson KE, Lux R, Shi W. 2015. Cultivation of a human-associated TM7 phylotype
553 reveals a reduced genome and epibiotic parasitic lifestyle. Proc Natl Acad Sci U S A 112:244-249.

554 12. Tian R, Ning D, He Z, Zhang P, Spencer SJ, Gao S, Shi W, Wu L, Zhang Y, Yang Y, Adams BG,
555 Rocha AM, Detienne BL, Lowe KA, Joyner DC, Klingeman DM, Arkin AP, Fields MW, Hazen
556 TC, Stahl DA, Alm EJ, Zhou J. 2020. Small and mighty: adaptation of superphylum
557 *Patescibacteria* to groundwater environment drives their genome simplicity. Microbiome 8:51.

558 13. Jaffe AL, Castelle CJ, Matheus Carnevali PB, Gribaldo S, Banfield JF. 2020. The rise of diversity
559 in metabolic platforms across the Candidate Phyla Radiation. BMC Biol 18:69.

560 14. Nales M, Butler BJ, Edwards EA. 1998. Anaerobic Benzene Biodegradation: A Microcosm Survey.
561 Bioremediation Journal 2:125-144.

562 15. Ulrich AC, Edwards EA. 2003. Physiological and molecular characterization of anaerobic benzene-
563 degrading mixed cultures. Environ Microbiol 5:92-102.

564 16. Luo F. 2016. Characterization of the Microbial Community Composition and Benzene Activation
565 Mechanisms in Anaerobic Benzene-Degrading Enrichment Cultures. PhD. University of Toronto,
566 TSpace.

567 17. Toth CRA, Luo F, Bawa N, Webb J, Guo S, Dworatzek S, Edwards EA. 2021. Anaerobic Benzene
568 Biodegradation Linked to the Growth of Highly Specific Bacterial Clades. Environ Sci Technol
569 55:7970-7980.

570 18. Luo F, Devine CE, Edwards EA. 2016. Cultivating microbial dark matter in benzene-degrading
571 methanogenic consortia. Environ Microbiol 18:2923-2936.

572 19. Guo S, Toth CRA, Luo F, Chen X, Xiao J, Edwards EA. 2022. Transient Oxygen Exposure Causes
573 Profound and Lasting Changes to a Benzene-Degrading Methanogenic Community. BioRxiv
574 doi:10.1101/2022.04.11.487956.

575 20. Griebler C, Lueders T. 2009. Microbial biodiversity in groundwater ecosystems. Freshw Biol
576 54:649-677.

577 21. Kocur CMD, Lomheim L, Molenda O, Weber KP, Austrins LM, Sleep BE, Boparai HK, Edwards
578 EA, O'Carroll DM. 2016. Long-Term Field Study of Microbial Community and Dechlorinating
579 Activity Following Carboxymethyl Cellulose-Stabilized Nanoscale Zero-Valent Iron Injection.
580 Environmental Science & Technology 50:7658-7670.

581 22. Suzuki S, Ishii SI, Wu A, Cheung A, Tenney A, Wanger G, Kuenen JG, Nealson KH. 2013.
582 Microbial diversity in The Cedars, an ultrabasic, ultrareducing, and low salinity serpentinizing
583 ecosystem. Proceedings of the National Academy of Sciences 110:15336-15341.

584 23. Anantharaman K, Brown CT, Hug LA, Sharon I, Castelle CJ, Probst AJ, Thomas BC, Singh A,
585 Wilkins MJ, Karaoz U, Brodie EL, Williams KH, Hubbard SS, Banfield JF. 2016. Thousands of
586 microbial genomes shed light on interconnected biogeochemical processes in an aquifer system.
587 Nat Commun 7:13219.

588 24. Thiel J, Byrne JM, Kappler A, Schink B, Pester M. 2019. Pyrite formation from FeS and H2S is
589 mediated through microbial redox activity. Proc Natl Acad Sci U S A 116:6897-6902.

590 25. Ulrich AC, Edwards EA. 2003. Physiological and molecular characterization of anaerobic benzene-
591 degrading mixed cultures. Environmental Microbiology 5:92-102.

592 26. Luef B, Frischkorn KR, Wrighton KC, Holman HY, Birarda G, Thomas BC, Singh A, Williams
593 KH, Siegerist CE, Tringe SG, Downing KH, Comolli LR, Banfield JF. 2015. Diverse uncultivated
594 ultra-small bacterial cells in groundwater. Nat Commun 6:6372.

595 27. Kuroda K, Yamamoto K, Nakai R, Hirakata Y, Kubota K, Nobu Masaru K, Narihiro T. 2022.
596 Symbiosis between Candidatus Patescibacteria and Archaea Discovered in Wastewater-Treating
597 Bioreactors. mBio 0:e01711-22.

598 28. Miyoshi T, Iwatsuki T, Naganuma T. 2005. Phylogenetic characterization of 16S rRNA gene
599 clones from deep-groundwater microorganisms that pass through 0.2-micrometer-pore-size filters.
600 Appl Environ Microbiol 71:1084-1088.

601 29. Poulsen LK, Ballard G, Stahl DA. 1993. Use of rRNA fluorescence in situ hybridization for
602 measuring the activity of single cells in young and established biofilms. Appl Environ Microbiol
603 59:1354-1360.

604 30. Beveridge TJ, Patel GB, Harris BJ, Sprott GD. 1986. The ultrastructure of *Methanothrix concilii*, a
605 mesophilic aceticlastic methanogen. Can J Microbiol 32:703-710.

606 31. Holmes DE, Shrestha PM, Walker DJF, Dang Y, Nevin KP, Woodard TL, Lovley DR. 2017.
607 Metatranscriptomic evidence for direct interspecies electron transfer between Geobacter and
608 Methanothrix species in methanogenic rice paddy soils. Applied and Environmental Microbiology
609 83.

610 32. Vigil-Stenman T, Ininbergs K, Bergman B, Ekman M. 2017. High abundance and expression of
611 transposases in bacteria from the Baltic Sea. The ISME Journal 11:2611-2623.

612 33. Vigil-Stenman T, Larsson J, Nylander JAA, Bergman B. 2015. Local hopping mobile DNA
613 implicated in pseudogene formation and reductive evolution in an obligate cyanobacteria-plant
614 symbiosis. BMC Genomics 16:193.

615 34. Walker A, Langridge G. 2008. Does my genome look big in this? Nature Reviews Microbiology
616 6:878-879.

617 35. Ran L, Larsson J, Vigil-Stenman T, Nylander JAA, Ininbergs K, Zheng W-W, Lapidus A, Lowry
618 S, Haselkorn R, Bergman B. 2010. Genome Erosion in a Nitrogen-Fixing Vertically Transmitted
619 Endosymbiotic Multicellular Cyanobacterium. PLoS ONE 5:e11486.

620 36. Van Melderen L, Saavedra De Bast M. 2009. Bacterial toxin-antitoxin systems: more than selfish
621 entities? PLoS Genet 5:e1000437.

622 37. Pandey DP, Gerdes K. 2005. Toxin–antitoxin loci are highly abundant in free-living but lost from
623 host-associated prokaryotes. Nucleic Acids Research 33:966-976.

624 38. Magnuson RD. 2007. Hypothetical functions of toxin-antitoxin systems. J Bacteriol 189:6089-
625 6092.

626 39. Craig L, Pique ME, Tainer JA. 2004. Type IV pilus structure and bacterial pathogenicity. Nature
627 Reviews Microbiology 2004 2:5 2:363-378.

628 40. Saier MH, Reddy BL. 2015. Holins in Bacteria, Eukaryotes, and Archaea: Multifunctional
629 Xenologues with Potential Biotechnological and Biomedical Applications. Journal of Bacteriology
630 197:7-17.

631 41. Peabody CR, Chung YJ, Yen M-R, Vidal-Ingigliardi D, Pugsley AP, Saier MH. 2003. Type II
632 protein secretion and its relationship to bacterial type IV pili and archaeal flagella. Microbiology
633 149:3051-3072.

634 42. Chen L-X, Al-Shayeb B, Méheust R, Li W-J, Doudna JA, Banfield JF. 2019. Candidate Phyla
635 Radiation Roizmanbacteria From Hot Springs Have Novel and Unexpectedly Abundant CRISPR-
636 Cas Systems. Frontiers in Microbiology 10.

637 43. de Luca G, de Philip P, Rousset M, Belaich JP, Dermoun Z. 1998. The NADP-Reducing
638 Hydrogenase ofDesulfovibrio fructosovorans:Evidence for a Native Complex with Hydrogen-
639 Dependent Methyl-Viologen-Reducing Activity. Biochemical and Biophysical Research
640 Communications 248:591-596.

641 44. Arnaouteli S, Giastas P, Andreou A, Tzanodaskalaki M, Aldridge C, Tzartos SJ, Vollmer W,
642 Eliopoulos E, Bouriotis V. 2015. Two Putative Polysaccharide Deacetylases Are Required for
643 Osmotic Stability and Cell Shape Maintenance in Bacillus anthracis. Journal of Biological
644 Chemistry 290:13465-13478.

645 45. Caufrier F, Martinou A, Dupont C, Bouriotis V. 2003. Carbohydrate esterase family 4 enzymes:
646 substrate specificity. Carbohydrate Research 338:687-692.

647 46. Psylinakis E, Boneca IG, Mavromatis K, Deli A, Hayhurst E, Foster SJ, Vårum KM, Bouriotis V.
648 2005. Peptidoglycan N-Acetylglucosamine Deacetylases from Bacillus cereus, Highly Conserved
649 Proteins in Bacillus anthracis. Journal of Biological Chemistry 280:30856-30863.

650 47. Vollmer W, Tomasz A. 2000. The pgdA Gene Encodes for a PeptidoglycanN-Acetylglucosamine
651 Deacetylase in Streptococcus pneumoniae. Journal of Biological Chemistry 275:20496-20501.

652 48. Tsigos I, Martinou A, Kafetzopoulos D, Bouriotis V. 2000. Chitin deacetylases: new, versatile tools
653 in biotechnology. Trends in Biotechnology 18:305-312.

654 49. Kafetzopoulos D, Martinou A, Bouriotis V. 1993. Bioconversion of chitin to chitosan: purification
655 and characterization of chitin deacetylase from Mucor rouxii. Proceedings of the National
656 Academy of Sciences 90:2564-2568.

657 50. Dörr T, Lam H, Alvarez L, Cava F, Davis BM, Waldor MK. 2014. A Novel Peptidoglycan Binding
658 Protein Crucial for PBP1A-Mediated Cell Wall Biogenesis in Vibrio cholerae. PLOS Genetics
659 10:e1004433.

660 51. Siewering K, Jain S, Friedrich C, Webber-Birungi MT, Semchonok DA, Binzen I, Wagner A,
661 Huntley S, Kahnt J, Klingl A, Boekema EJ, Søgaard-Andersen L, van der Does C. 2014.
662 Peptidoglycan-binding protein TsaP functions in surface assembly of type IV pili. Proceedings of
663 the National Academy of Sciences 111:E953-E961.

664 52. Kantor RS, Wrighton KC, Handley KM, Sharon I, Hug LA, Castelle CJ, Thomas BC, Banfield JF.
665 2013. Small genomes and sparse metabolisms of sediment-associated bacteria from four candidate
666 phyla. mBio 4:e00708-13.

667 53. Faust K, Raes J. 2016. CoNet app: inference of biological association networks using Cytoscape.
668 F1000Research 5:1519.

669 54. Raskin L, Poulsen LK, Noguera DR, Rittmann BE, Stahl DA. 1994. Quantification of
670 methanogenic groups in anaerobic biological reactors by oligonucleotide probe hybridization. Appl
671 Environ Microbiol 60:1241-1248.

672 55. Toth CRA, Molenda O, Nesbø CL , Luo F, Devine C, Guo S, Chen X, Edwards EA. 2023.
673 Metagenomic and Genomic Sequences from a Methanogenic Benzene-Degrading Consortium.
674 Microbiology Resource Announcements – MRA01342-22 - Submitted Dec 20, 2022. In review

675

676 **Figure and Legends**
677

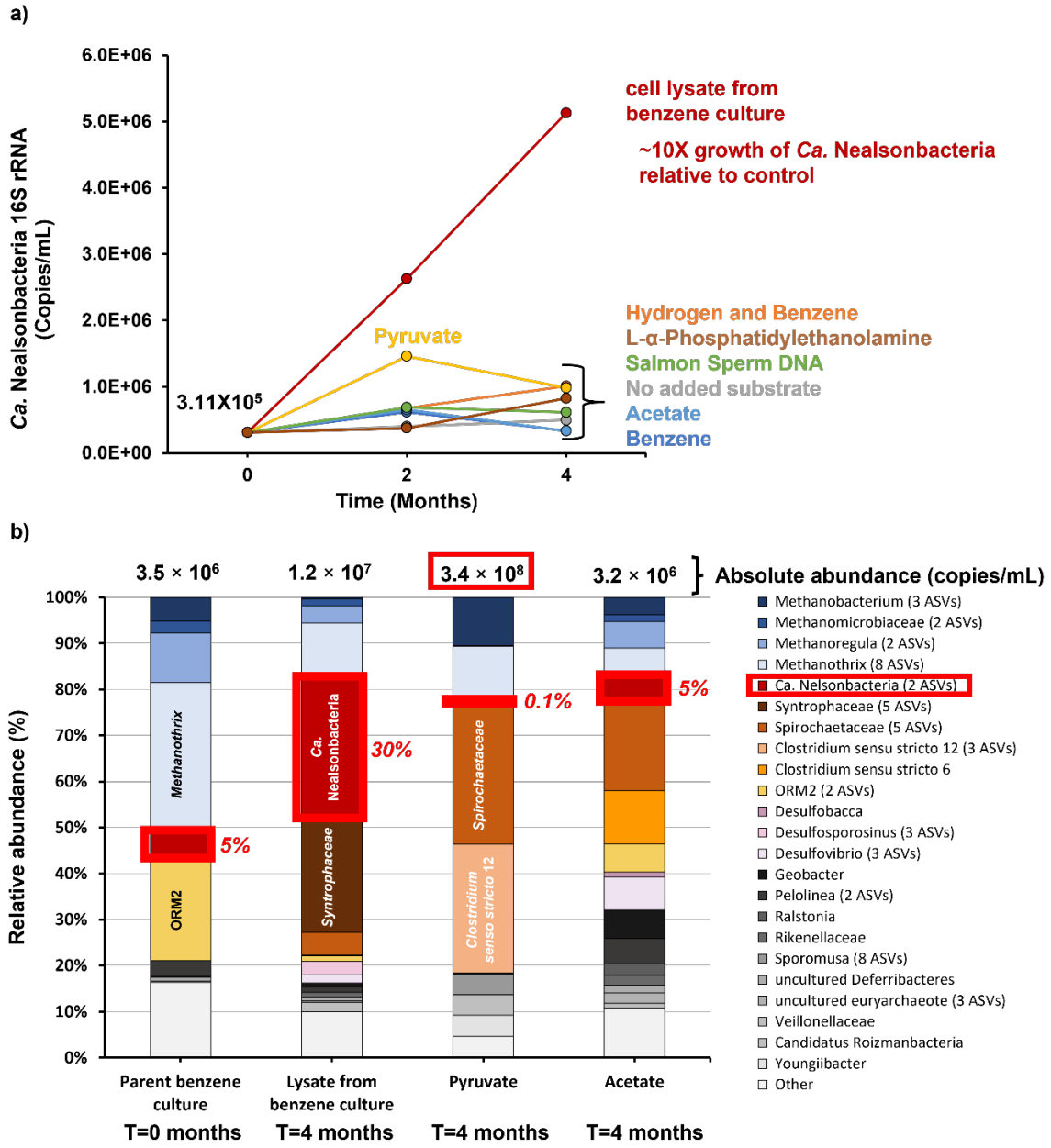

678
679 **Figure 1. Results of Growth Trial #1.** a) Absolute *Ca.* Nealsonbacteria abundance measured by
680 qPCR in copies/mL, and b) microbial community profiles (relative abundance) as a function of
681 substrate after 4 months of incubation, with total abundance shown above bars. In panel a) one
682 DNA sample was collected on day 1 to represent initial conditions. Subsequent DNA samples were
683 collected by sacrificing one entire bottle at each time point for each treatment due to the limited
684 culture volume. In panel b) ASVs with relative abundances < 1% were combined as "Other". ASVs
685 with the same taxonomy at the genus level were combined. The number of combined ASVs for
686 each taxon is shown in brackets. Absolute abundance was obtained by adding the qPCR results for
687 total bacteria, total archaea and *Ca.* Nealsonbacteria together. "Parent Benzene culture" column is
688 a 10% transfer of the parent culture at time zero.

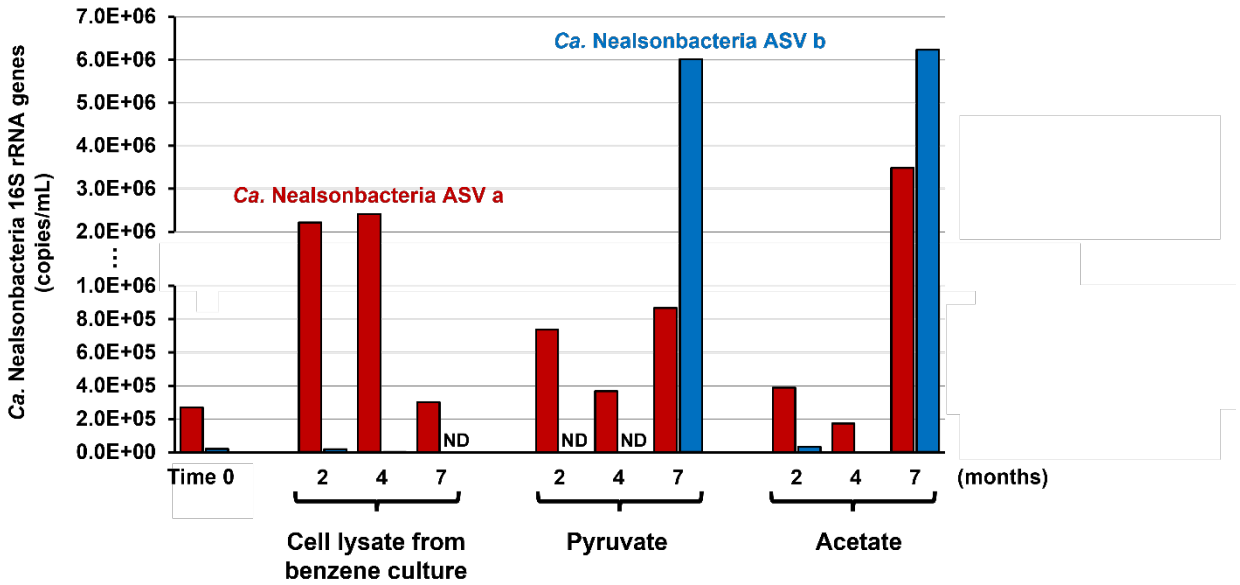

Figure 2. *Ca.* Nealsonbacteria strain abundance over 7 months of incubation. Figure shows treatments amended with benzene culture lysate, acetate, or pyruvate from Donor Trial #1. DNA samples were collected by sacrificing one entire bottle at each time point for each treatment due to the limited culture volume. Absolute abundance of *Ca.* Nealsonbacteria strains ASVa and ASVb were calculated by multiplying the relative abundance of these ASVs (obtained from amplicon sequencing) by the absolute abundance of total bacterial.

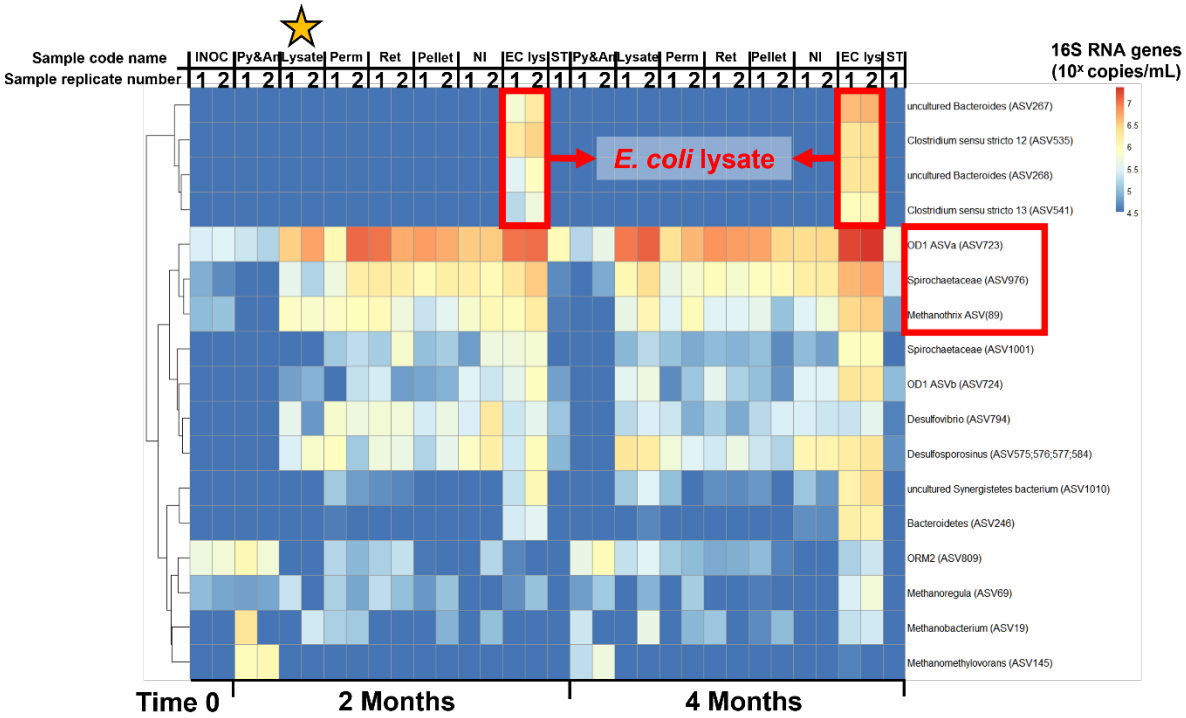

Figure 3. Heatmap of absolute abundance of top 20 ASVs in growth Trial #2. Top 20 ASVs were selected based on the sum of absolute abundance across all DNA samples collected. The ASVs under *Desulfosporosinus* are combined. Rows were clustered using a hierarchical clustering algorithm "hclust" in R based on similarity of absolute abundance. The columns represent different treatment bottles: INOC: Bottle with only 10% inoculum at time 0; NI: no inoculum (lysate only); Py&An: pyruvate & antibiotics; Lysate: French pressed benzene culture; Perm: lysate supernatant permeate through 50 kDa membrane; Ret: lysate supernatant retentate; Pellet: lysate pellet after centrifugation at 13,000 x g for 20 min; EC lys: French pressed lysate of *E. coli* culture; ST: Starved culture. The bracketed ASV numbers in the row names represent ordinal ASV number (see Table S3).

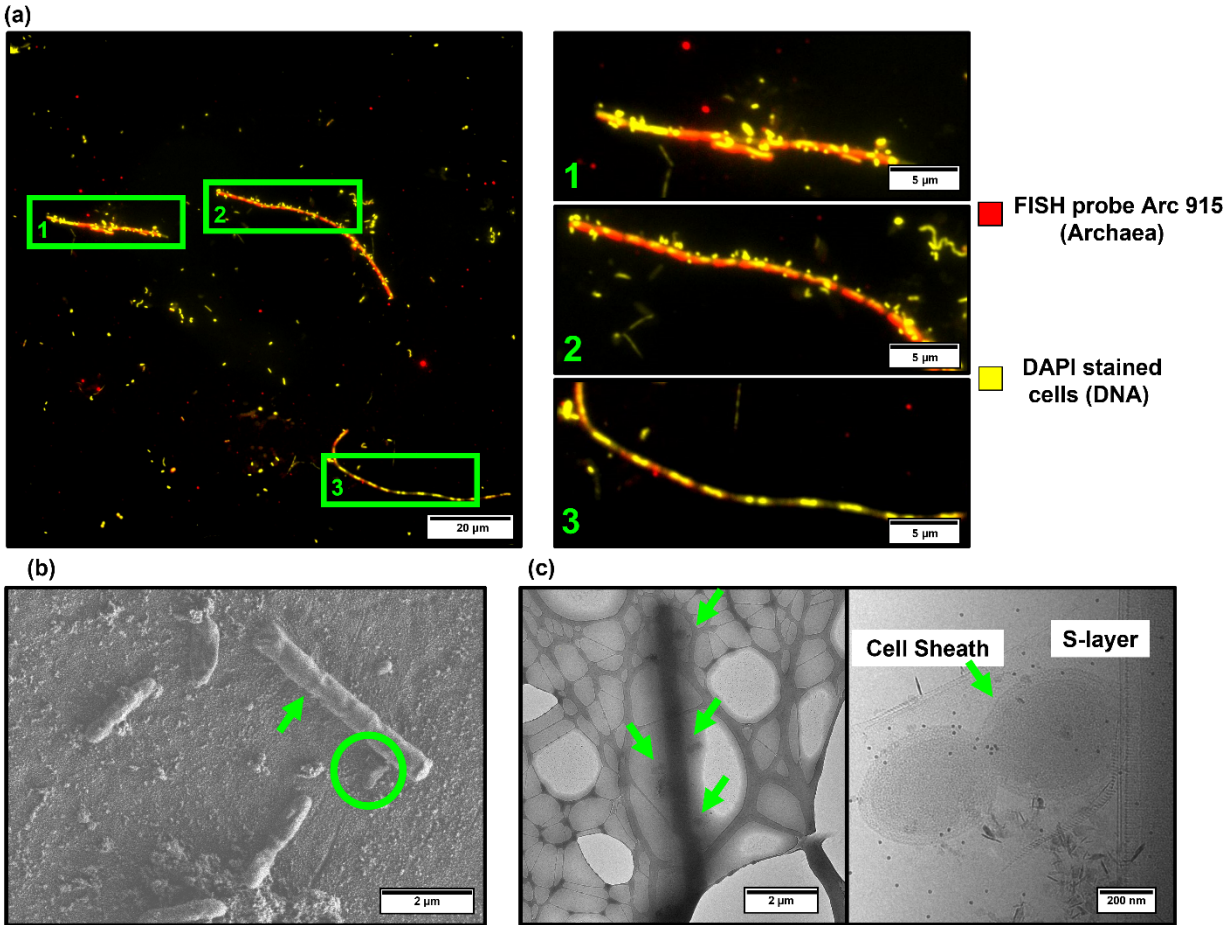

Figure 4. Various microscopic images of *Ca.* Nealsonbacteria in enrichment cultures. (a) Epifluorescence microscopy showing archaea (red) and DAPI (yellow). Images are false colored and overlaid using ImageJ. Images on the right are zoomed in views of green rectangular area in the left image highlighting archaeal filaments with and without attached cells. (b) SEM images of methanogenic benzene-degrading culture prepared by ionic liquid exchange. A *Methanothrix* filament is marked with green arrow. *Ca.* Nealsonbacteria-like cells are marked with a green circle. (c) Cryto-TEM images of *Ca.* Nealsonbacteria enrichments. *Ca.* Nealsonbacteria-like cells are marked by green arrows and the right-side shows a zoomed in view of two cells that appear to be budding. Additional microscopic images are shown in Figures S5 and S6.

(a) Cumulative benzene degraded

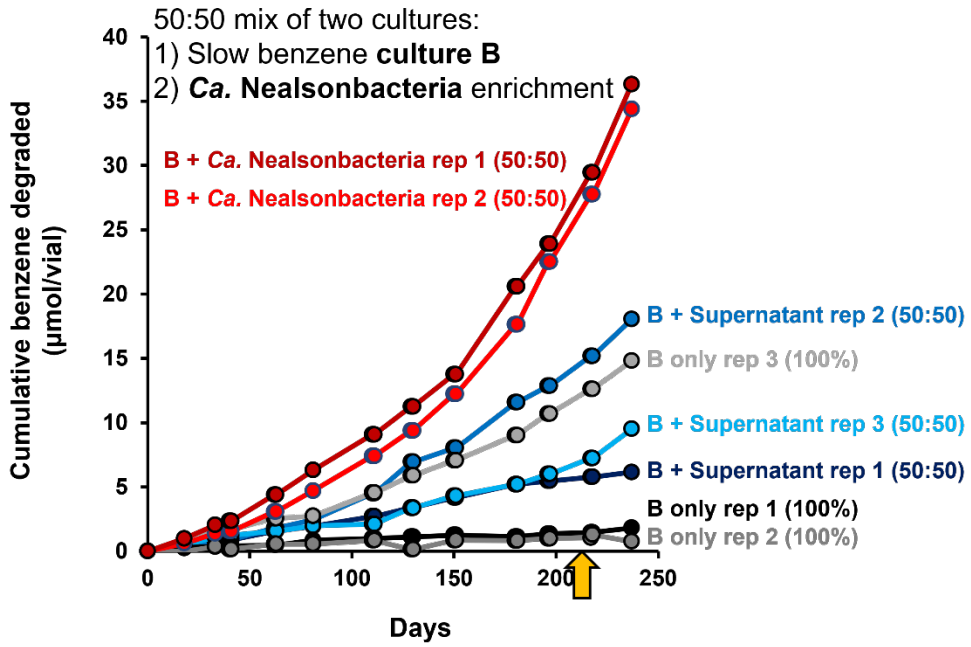

(b) qPCR results on Day 217

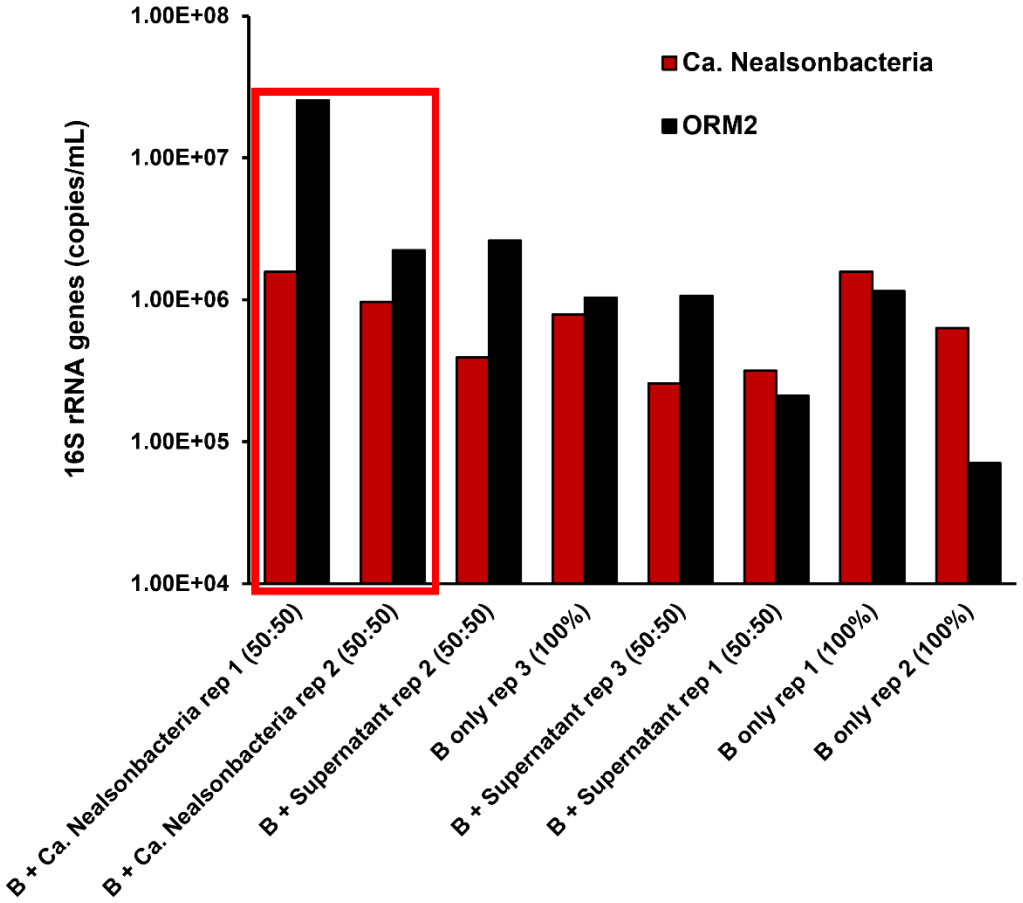

726

727
728 **Figure 5. Impact of adding *Ca.* Nealsonbacteria enrichment to a slow benzene-degrading**
729 **culture**. a) Cumulative benzene consumption and b) qPCR results tracking *Ca.* Nealsonbacteria
730 and ORM2 on Day 217. The qPCR results are sorted by descending order of benzene degradation
731 rate. The biological replicates are plotted separately to show the differences.
732
733
734
735
736

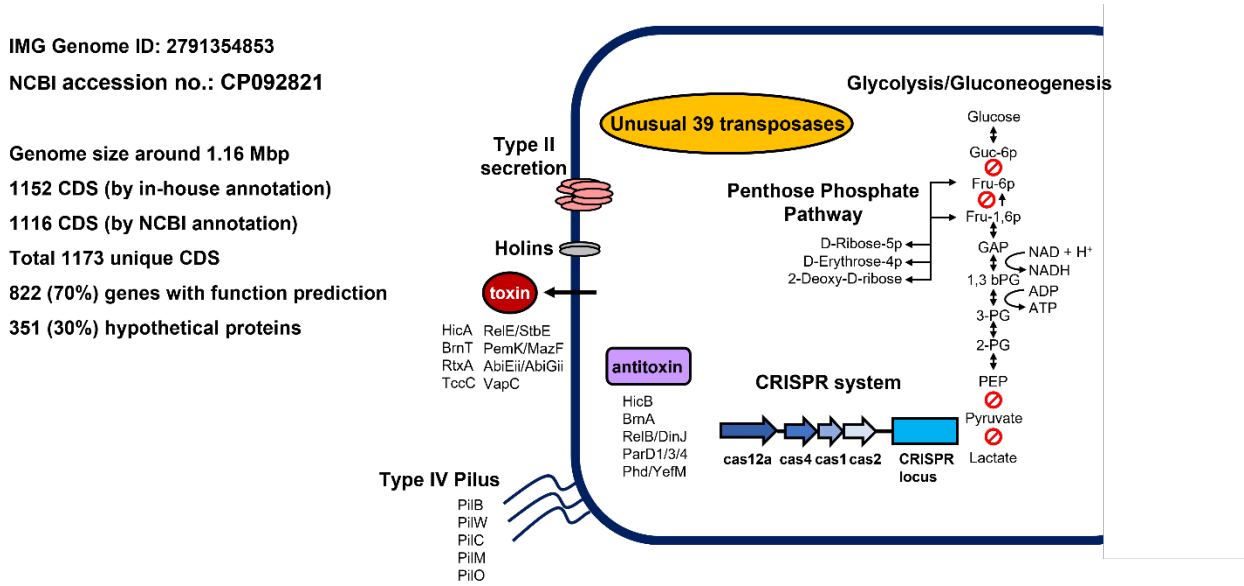

737
738
739 **Figure 6. A summary of key findings from the genome of *Ca.* Nealsonbacteria DGGOD1a**.
740 Detailed annotations for each ORF are in Table S10.
741
742
743
744
745 **AUTHOR CONTRIBUTIONS**

746 All authors made research and substantial intellectual contributions to the completion of this
747 study. X.C. and E.A.E. conceived and designed the study, and X.C carried out all experiments,
748 data analysis and interpretation, and drafted and revised the manuscript. O.M. assembled the
749 OD1 genome with help of C.N. and C.T.B. L.M performed the Cryo-TEM data acquisition and
750 analysis. C.R.A.T. helped with data analysis and revised the manuscript. S.G. helped to maintain
751 the culture, performed qPCR data acquisition and analysis and revised the manuscript. F.L.
752 enriched the culture, extracted DNA and performed the initial metagenome analysis. J.H. assisted
753 with ionic liquid-SEM data acquisition and analysis. C.H. performed the OD1 taxonomy
754 classification, phylogenetic tree and OD1 genome annotation. J.H.D.C. and J.F.B. provided
755 critical research guidance, and manuscript revisions.
756